Preprint version.
Accepted after revision by ACS Biomaterials Science & Engineering
https://doi.org/10.1021/acsbiomaterials.2c01391

Potential of a plasma-aerosol system for wound healing advanced by drug introduction: an *in vitro* study

Ivana Sremački[a], Mahtab Asadian [a,b], Nathalie De Geyter[a], Christophe Leys[a], Liesbet Geris[b,c], Anton Nikiforov[a]

[a] Department of Applied Physics, Ghent University, Gent 9000, Belgium

[b] Skeletal Biology & Engineering Research Center, 3000 Leuven, Belgium

[c] Biomechanics Research Unit, GIGA In Silico Medicine, Liège University, 4000 Liège, Belgium

Abstract

Cold plasmas have found their application in a wide range of biomedical fields by virtue of their high chemical reactivity. In the last decades, many attempts have been made to use cold plasmas in wound healing and within this field many studies have focused on plasma-induced cell proliferation mechanisms. In this work, one step further has been taken to demonstrate the advanced role of plasma in wound healing. To this end, the simultaneous ability of plasma to induce cell proliferation and permeabilize treated cells has been examined in the current study. The driving force was to advance the wound healing effect of plasma with drug delivery. On this subject, we demonstrate *in vitro* the healing effect of Ar, Ar+N_2 plasma, and their aerosol counterparts. A systematic study has been carried out to study the role of ROS and RNS (RONS) in cell adhesion, signaling, differentiation, and proliferation. An additional investigation was also performed to study the permeabilization of cells, and the delivery of the modeled drug carrier FITC labeled dextran into cells upon plasma treatment.

Short 35 s plasma treatments were found to promote fibroblast adhesion, migration, signaling, proliferation, and differentiation by means of RONS created by plasma and deposited into the cell environment. The impact of the plasma downstream products NO_2^- and NO_3^- on the expressions of the focal adhesion's genes, syndecans and collagens was observed to be prominent. On the other hand, the differentiation of fibroblasts to myofibroblasts was mainly initiated by ROS produced by the plasma. In addition, the ability of plasma to locally permeabilize fibroblast cells was demonstrated. During proliferative cell treatment, plasma can simultaneously induce cell membrane permeabilization (d~7.3 nm) by the species OH and H_2O_2. The choice for a plasma or a plasma-aerosol configuration thus allows the possibility to change the spatial chemistry of drug delivery molecules and thus to locally deliver drugs. Accordingly, this study offers a pivotal step toward plasma-assisted wound healing advanced by drug delivery.

1. Introduction

Normal healing of a wound can be described by four time-overlapping but distinct phases, namely hemostasis, inflammation, proliferation (re-epithelization, neovascularization, tissue granulation), and remodeling. In a normal wound upon skin injury, fibroblasts are activated, migrate into the damaged tissue, adhere to the provisional extracellular matrix (ECM), and proliferate[1]. In the remodeling phase, the ECM is rearranged, and transforming growth factor-beta (TGF-β) induces fibroblast differentiation into myofibroblasts[2]. Depending on the patient's history and condition, some healing steps can be prolonged or shifted, and abnormal or chronic wounds may develop. Abnormal or chronic wounds seem to be a global problem impacting the population worldwide, as suggested by the growing number of diabetic patients (~20% increase in 10 years)[3].

Advanced techniques developed in the field of regenerative medicine rely on wound oxygenation[4] and nitration[5] (hyperbaric oxygen chamber, radiofrequency (RF) electromagnetic field stimulation). Bioengineered therapies have also recently received considerable attention from the healthcare sector. The most promising of these are cellular[6] and acellular, e.g., ECM- and growth factor (GF)-based therapies[7]. Although some clinical treatments are available (6 000-10 000 euro/annually[8]) for the wound healing process, reliable solutions with conspicuous success for diabetic foot ulcers (DFU) remain elusive. Therefore, alternative approaches that are just as effective as the current approaches are desired.

Over the past two decades, researchers have developed the concept of redox control in wound healing which has offered new hope of providing effective therapies in this field[9]. The development was based on the assumption that reactive oxygen species (ROS), especially superoxide (O_2^-) and hydrogen peroxide (H_2O_2), boost the release of vascular endothelial growth factor (VEGF), stimulating epithelialization and collagen deposition during the proliferation and remodeling phase, and thereby promoting wound healing[10]. Over the following years, several reactive species-related wound healing processes have been elaborated, and evaluations of these processes have indicated that controlled production and release of ROS and reactive nitrogen species (RNS) promotes wound healing[11].

To this end, cold atmospheric plasmas (CAPs) exhibit significant potential for use in wound healing[12-13]. CAPs are chemically reactive media, which produce charged particles, metastables, radicals, reactive oxygen and nitrogen species (RONS), and ultraviolet (UV) radiation[12]. The biomedical application of atmospheric pressure plasmas is often associated with their RONS production and is explained by redox biology[14]. RONS-induced changes in intracellular chemistry are critical for cell homeostasis and signaling including energy metabolism, gene expressions, immune responses, cell cycles, growth (GF and TGF- β1 release[15]), and apoptosis[16]. Biological effects of plasmas have been studied globally, and their coagulative[17], antibacterial[18-19], and proliferative effects have been revealed[20-22]. These attributes suggest that CAPs should be excellent candidates for alternative wound care technologies[13, 23]. Although the wound healing potentials of many CAPs have been confirmed *in vitro, in vivo*, and in clinical trials, the role of RONS from plasmas remain unclear and must be addressed. Accordingly, additional investigations of RONS healing pathways are highly desired.

In previous studies, a certified plasma jet was employed for the randomized treatment of diabetic rat wounds[24]; however, the best performances were realized when plasma treatment was combined with bioactive agents (hyaluronic acid and collagen). These results proved the positive effect of combining plasma jets with drug delivery systems and thus the importance of designing a plasma jet to synergistically enhance wound healing and locally deliver drugs. Topical and transdermal drug delivery techniques (e.g., electroporation, iontophoresis) are already abundantly used to enhance and induce delivery of molecules through the stratum corneum (15 µm), epidermis and dermis (d~2 mm) to blood vessels[25-26]. In the past two decades, electroporation[27] is employed clinically to deliver chemotherapeutics[28], and genes (DNA vaccine and RNA transfection[29]) through skin. Topical delivery of drugs via electroporation is highly effective but is unfortunately inapplicable to patients with pacemakers or those undergoing anticoagulant therapy.

In this study, new potentials of an atmospheric pressure plasma jet (APPJ) are highlighted to resolve the existing issues concerning plasma-promoted wound healing advanced with drug delivery. The design and biomedical aspects of an APPJ coupled with aerosol have been previously studied utilizing physical[30], chemical[31], and biological[32] diagnostics. The advantages of an APPJ coupled with aerosol include its high stability, its low temperature, and its ability to manipulate the RONS and UV radiation flux toward the biomaterial, thereby enabling safe and controlled medical treatment. Accordingly, in the current work, we study plasma-advanced healing *in vitro*, concretely plasma-assisted connective tissue fibroblast cell proliferation, and controlled drug introduction in treated cells. In the simplified *in vitro* wound healing model, we demonstrate the potential of an APPJ to enhance fibroblast proliferation and cell permeabilization for drug delivery. The fibroblast viability and proliferation rate after plasma treatment have been determined via staining and colorimetric assays. In addition, the expression of the most crucial genes in wound healing after plasma treatment of fibroblast cells has been investigated through quantitative real-time polymerase chain reaction (qRT-PCR). Accordingly, the expression of upregulating genes associated with migration, adhesion, cell-cell/matrix signaling, and fibroblast differentiation

toward myofibroblasts has been evaluated post plasma treatment. Nitrogen gas (N_2) has also been added to the feeding gas argon (Ar) to investigate the biological effect of RNS in wound healing in the *in vitro* models. Emphasis is given to the potential role of the APPJ in fibroblast-cell permeabilization and the local introduction of a drug carrier (dextran).

2. Materials & methods

In this work, the wound healing aspects of an APPJ coupled with aerosol have been studied *in vitro.* The plasma jet reactor used for this purpose is a large size (d_{out}=14 mm) annular-shaped device. A cylindrical, hollow, powered electrode (RF 13.56 MHz) is built in the grounded body of the reactor. When a high voltage is applied between the two cylindrical electrodes and 3 SLM (standard liter per minute) of Ar is used, plasma is generated in an annular shape between the electrodes and a plasma jet is formed in ambient air, as presented in Figure 1 (left). A detailed description of the employed plasma reactor can be found in previous work[30].

Through the hollow electrode, aerosol microdroplets (d~20μm) of water can be introduced into the plasma effluent for RONS and UV flux modification towards the target, as presented in Figure 1 (right). In this work, water microdroplets are introduced with a flow rate of 100 ul/min ($3x10^5$ droplets/s). Moreover, the plasma-initiated chemistry in the gas and liquid phase can also be modulated to a certain extent by adding other gases to the feeding gas Ar. In this study, 0.05% is added to Ar to boost the generation of RNS. An overview of the influence of water microdroplets in the plasma jet and the presence of N_2 in the plasma feeding gas on RONS chemistry is given in the following section.

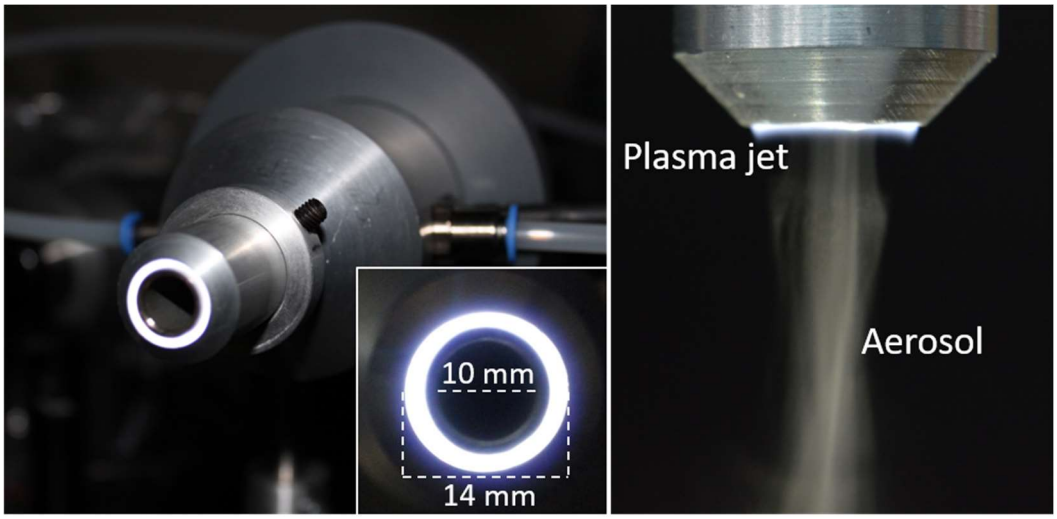

Figure 1. Image of the RF annular shape plasma reactor with the enlarged cross-section of the plasma ring (left); enlarged image of the plasma nozzle and the plasma jet coupled with aerosol (right).

2.1. Manipulation of RONS production in plasma treatments: adding N_2 and water aerosol

The APPJ sustained in Ar and coupled with water aerosol employed in this work has been designed for plasma-assisted wound healing[30-32]. Previous studies have shown that oxygen-driven ROS chemistry and UV radiation photo-induced chemistry are dominant in this jet. The liquid chemistry initiated by the APPJ and the possibility of modifying ROS species generation/deposition by adding water aerosol to the plasma effluent has previously been investigated[31]. The RONS generated in a plasma-treated liquid (water or phosphate-buffered saline (PBS)) play a crucial role in the *in vitro* studies, considering that the liquid layer always covers the cells. The addition of aerosol can spatially modify the RONS production and deposition and, accordingly, manipulate the plasma interface[32]. Moreover, due to partial ROS quenching and UV absorption, the biological effects of aerosol addition mirror safer treatments.

The ROS production in the applied APPJ can also be modified by adding N_2 to the Ar feeding gas. A low amount (0.05%) of N_2 does not affect the stability and temperature of the plasma jet[30]. However, boosted

production of RNS (RONS) is apparent. The addition of nitrogen gas favors NO production in the gas phase and downstream reaction products NO_2^- and NO_3^- in the liquid phase (see Table 1)[33]. For these purposes, hydroxyl radicals (OH), atomic oxygen (O), and superoxide (O_2^-) are directly or indirectly consumed for nitrate and nitrite ions production[34]. The positive effects of the Ar jet on angiogenesis, blood flow in the wound, epithelization, and wound contraction is closely related to a higher concentration of RNS (RONS) in a wound bed[35]. Biologically crucial RONS produced in the treated liquid have been measured before in *in vitro* studies. An overview of the dominant species produced by the APPJ in liquid (PBS) treated at a distance of 10 mm is given in Table 1.

Table 1. RONS produced or deposited to treated PBS by the APPJ (d=10 mm, t=10-60 s)

Plasma	OH	O_2^-	H_2O_2	NO_2^-	NO_3^-
Ar	0.5-2.8 uM	0.2-1.8 uM	4.0-2.0 uM	1.0-2.0 uM	5.0-3.0 uM
Ar+N_2	↘	↘	↘	↗	↗
Ar-aerosol	0.5-2.0 uM	0.1-1.2 uM	1.0-3.0 uM	1.0 uM	2.0-1.0 uM
Ar+N_2-aerosol	↘	↘	↘	↗	↗

Focusing on the long-living species (H_2O_2, NO_2^-, and NO_3^-) concentrations, the addition of N_2 to the carrier gas Ar results in a decrease in H_2O_2 concentration below 2 uM, while the concentration of NO_2^- increase to 3.5 uM. Adding aerosols to the Ar+N_2 plasma even further enhances the generation of nitrites to 4 uM. Accordingly, the small addition of N_2 gas to the plasma jet will selectively quench or boost the generation of ROS and RNS, so the effect of the plasma jet on fibroblast cells can be tuned in terms of RONS concentrations.

2.2.1.Plasma treatment of fibroblast cells

This research focuses on promoting the healing of a chronic wound by using a cold plasma jet. Hereby, an additional perspective of the plasma jet has been investigated that could be advantageous in future applications. Precisely, besides studying the healing effect of the plasma jet solely, particular interest was given to the possibility of permeabilizing cells by plasma and introducing drugs. Consequently, fibroblast cells of an L929 cell line have been treated in a cell medium to study the plasma impact on:

I. Cell viability, proliferation, and gene expressions concerning migration, adhesion, signaling, and differentiation, respectively.
II. Cell permeabilization and model drug introduction into fibroblast cells.

Cells were treated at a 10 mm distance from the plasma effluent using a low power ($P_{dissipated}$=7 W) pure Ar, Ar+0.05% N_2, Ar-aerosol, and Ar+N_2-aerosol plasma. Short treatment times were defined in advance to be 10 s, 35 s, and maximal 60 s. The methodology of the performed experiments to study plasma wound healing and drug introduction *in vitro* is presented in Figure 2. Visualization of the plasma-produced species and the plasma exposure of the fibroblasts is shown in Figure 2 (a).

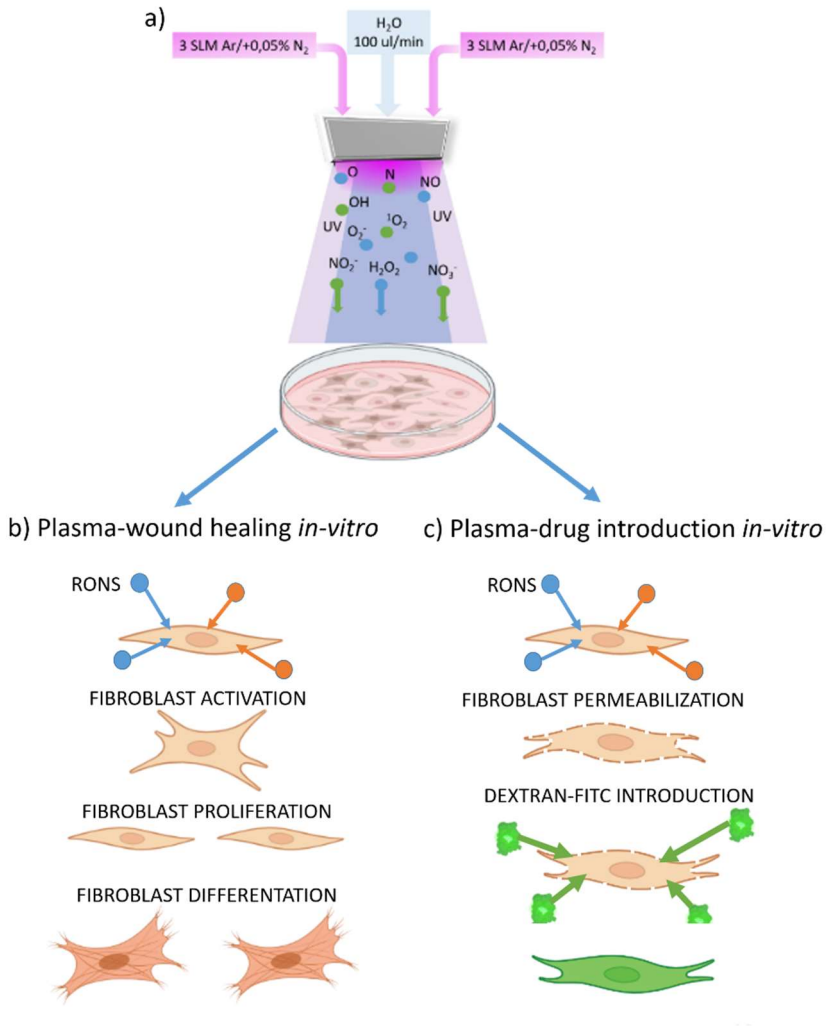

Figure 2. Experimental methodology defined to study plasma-wound healing and drug delivery *in vitro*: a) Schematic of the plasma treatment of fibroblast cells; b) Schematic of the plasma interactions with fibroblasts promoting their proliferation and differentiation; c) Schematic of the plasma interactions with fibroblasts inducing their permeabilization and dextran introduction.

The interactions of plasma with fibroblasts were studied through their proliferation and differentiation, as shown in Figure 2 (b). For this purpose, plasma-treated cells were subjected to different colorimetric and staining assays to study their proliferation and viability after the treatment. Moreover, expressions of genes relevant to wound healing are also measured by qRT-PCR. Ultimately, the cell permeabilization upon interaction with plasma was studied as presented in Figure 2 (c). A typical drug carrier, FITC (fluorescein isothiocyanate) labeled dextran, was used as a staining molecule. This biopolymer does not penetrate cells freely, but only when those are permeabilized.

2.2.2. Cell culture and preparation of samples

The L929 murine fibroblasts (American Type Culture Collection, Manassas, VA, USA) were cultured in an advanced minimum essential medium (AMEM; Gibco, Thermo Fisher Scientific), supplemented with 5% fetal bovine serum (FBS; Thermo Fisher), 10 mL/L L-glutamine (GlutaMAX; Thermo Fisher), 100 U/mL penicillin and 50 µg/mL streptomycin (Sigma Aldrich) in a 5% CO_2 humidified incubator at 37°C. In the next step, 1 x 10^6 L929 cells were suspended in 1.5 mL cell medium (AMEM) to assure uniform plasma treatment without spillage due to the employed gas flow. After the plasma treatment, 1000 L929 cells from each experimental group were plated in 0.1 mL cell culture medium in 96-well plates. All experiments were repeated three times and from each

experimental group, two replicates were sampled. Cells were incubated at 37°C in a 5% CO_2 humidified incubator for up to 7 days.

2.3. Cell viability and proliferation study: Presto Blue colorimetric assay and live/dead staining

The proliferative plasma effect on the L929 murine fibroblasts viability was studied using two different methods: a quantitative method (a Presto Blue assay) and a qualitative method (Live/dead staining). The cells are treated at a 10 mm distance from the plasma jet for 10, 35, and 60 s with Ar and Ar+N_2 plasma with and without aerosol. All samples are analyzed 1, 3, and 7 days after the treatment.

In the quantitative proliferative study, 10 µL of Presto Blue® viability reagent (Thermo Fisher Scientific) was added to the wells. Two hours later, the fluorescence intensity was measured with a microplate reader (Cytation 1, BioTek Instruments), from which cell viability could be determined. The cell proliferation of the experimental groups was normalized to the untreated control group on a corresponding day. As a complementary evaluation of cell viability in addition to morphology visualization, a live/dead viability/cytotoxicity kit (Invitrogen) was used. Prior to the staining, the supernatant was removed, and the cells were rinsed twice with PBS. Next, the staining was done by incubating the cells in the staining solution (0.5 µL 4 mm Calcein AM in anhydrous dimethyl sulfoxide DMSO solution and 2 µL 2 mm ethidium homodimer in DMSO: H_2O (1:4 v/v) in 1 mL PBS) for 20 min at room temperature in the dark. Finally, the cells were visualized with a fluorescence microscope (Olympus IX 83) using appropriate filters.

2.4. Expression of genes crucial to wound healing - *in vitro* study

The eventual goal of this study was to investigate the mechanism governing the effect of RONS-generating plasma on the wound healing process. The capacity of the generated RONS to boost the differentiation of cells was quantified via qRT-PCR 6 h, 24 h, and 48 h after conducting a 35 s plasma treatment. Total RNA from the L929 fibroblast cells was extracted utilizing the Nucleospin RNA II kit (Macherey-Nagel). The total RNA was isolated using QIAshredder (Qiagen) and continued by the RNeasy Mini Kit (Qiagen). This analysis was performed using at least three replicates per condition. RNA quality and concentration were evaluated with NanoDrop 2000 (Thermo Scientific), and the PrimeScript™ RT reagent kit (Takara) was utilized for cDNA synthesis. qRT-PCR was carried out utilizing SYBR® Green (Life Technologies) with Rotor Gene® 6000 (Qiagen), and relative differences in expression were measured using the $2^{-\Delta\Delta Ct}$ method normalized to the housekeeping gene glyceraldehyde-3-phosphate dehydrogenase (GAPDH)[36]. All protocols were performed according to the manufacturer's protocol. Using qRT-PCR, the most crucial gene expressions in the wound healing steps were examined. Cell surface-adhesion complexes measured hereby are involved in cytoskeletal organization and cell signaling mechanisms. Accordingly, these genes are crucial in maintaining attachment to ECM through a group of focal adhesion proteins, namely paxillin α (PXNα), focal adhesion kinase (FAK), talin (TLN), vinculin (VCL), and via syndecans transmembrane proteins connected to ECM (SCD1,4). Moreover, the expression of ECM protein-collagens (COL 1A1, IV), cell-proliferation index (Ki-67), and fibroblast differentiation α-smooth muscle actin (αSMA) were also examined. Further details are provided in Table S1 (SI).

2.5. Cell permeability measurements: Labeled FITC dextran introduction and detection

Labeled dextran-FITC 4, 10, 40, and 70 kDa (Sigma Aldrich) was used to evaluate the permeabilization of the fibroblasts upon plasma treatment. The optimal concentration of the dextran-FITC solution in PBS has been determined at 37.5 mg/mL for fluorescence microscopy of stained cells. For these cell permeabilization experiments, 10^5 L929 fibroblast cells were first seeded 1 day before plasma exposure into 6-well plates to reach a confluence of 80-90% (examined with a light microscope). Culturing and incubation of the cells were done as explained above. Prior to the plasma treatment, the cell medium was removed, and 500 uL of a 1:1 dextran/phenol red-free medium (MEM, Gibco, Thermo Fisher) 18.75 mg/mL solution was added[37]. The cultured fibroblasts with dextran present in the cell medium were subsequently treated at a distance of 10 mm with Ar, Ar+0.05% N_2, Ar-aerosol, and Ar+N_2-aerosol plasma. After 35 s of plasma treatment, 1.5 mL of fresh AMEM medium was added to the cells, after which dextran together with the cell medium was removed, and the cells were rinsed 3 times with 1.5 mL of fresh AMEM medium. Immediately after plasma treatment, the fluorescence

of the dextran penetrating into the cells was detected by fluorescence microscopy (Olympus IX 83) with the maximum at the wavelength of 519 nm using the mosaic style and 4x magnification. Control samples, which were treated 35 s with the plasma feeding gas flow but without switching on the plasma and following the same rinsing protocol, were examined as well.

2.6. Statistical analysis

All results will be presented as a mean value, including the corresponding error bars. One-way ANOVA (t-test) statistical analysis has been performed in GraphPad Prism 9 (GraphPad Software, Inc., CA, USA) to determine statistically significant differences between experimental groups. Significance levels $P<0.05$ (*), $P<0.01$(**), $P<0.001$(***), and $P<0.0001$(****) have been tested among all experimental groups.

3. Results & discussion

In this work, different aspects of plasma-assisted wound healing are demonstrated *in vitro*. In a first step, connective tissue fibroblast cells are treated with plasma (in the presence/absence of aerosol), as previously explained. Afterwards cell viability and proliferation are measured by live/dead staining and a quantitative colorimetric assay. Additionally, processes triggered in fibroblast proliferation and/or differentiation during a tissue injury and their consequent behavior are also examined by measuring relevant gene expressions after plasma treatment. Moreover, the innovative approach of combining plasma with localized drug delivery into the plasma-treated fibroblasts is also investigated. The driving force of this study was to boost the already well-investigated healing effect of plasma solely and combine it with drug delivery. Accordingly, the first study focuses on the proliferative character of plasma exclusively. Respectively, the second study investigates the local permeabilization of cells utilizing plasma as the first step toward commercialized plasma-assisted wound healing and drug delivery.

3.1. Fibroblast viability and proliferation after plasma treatment – wound healing: *in vitro* model

Based on our previous investigations[32], the fibroblast proliferation rate increases after cells are treated less than 60 s with the plasma effluent of a low power ($P_{dissipated}$=7 W) APPJ sustained in Ar and Ar-aerosol at distances of 5, 8 and 12 mm. Short exposure to Ar and Ar-aerosol plasma is therefore considered safe and non-toxic for the L929 cell line. On the opposite, the same study demonstrated cytotoxic effects on the fibroblasts when cells were overexposed to the same APPJ in Ar for a longer time, e.g., 120 and 240 s[32]. This was due to the excess amounts of RONS produced during longer plasma exposures resulting in a cytotoxic effect on fibroblasts. This negative impact has been explained by strong oxidative stress resulting from high concentrations of ROS (e.g., H_2O_2) and the disability of the cells to adapt to the highly oxidative environment while entering temporary or permanent growth arrest and apoptosis[38]. This undesirable behavior is less prominent in the aerosol-containing plasma systems than in the non-aerosol systems, indicating that the aerosol likely provides a cushioning effect for the cells by modulating the oxidation environment[31].

In this study, a Presto Blue assay was utilized to examine the fibroblast cell proliferative behavior upon plasma treatment in various carrier gases and in the presence/absence of aerosol (Ar, Ar+N_2, Ar-aerosol, and Ar+N_2-aerosol). The obtained results are compared with those of the untreated sample (ctrl) as shown in Figure 3 (a), while Figure 3 (b) demonstrates the proliferation only for the plasma treatment time of 35 s normalized on the control sample of the first day. The cell proliferation after 35 s treatment presented in Figure 3 (b) gives an overview of the cell proliferation during the monitoring days and the exponential growth of the cells. The fluorometric Presto Blue assay was selected, as according to literature, this new, simple, and fast assay is considered a highly sensitive assay for monitoring cell viability and cytotoxicity[39].

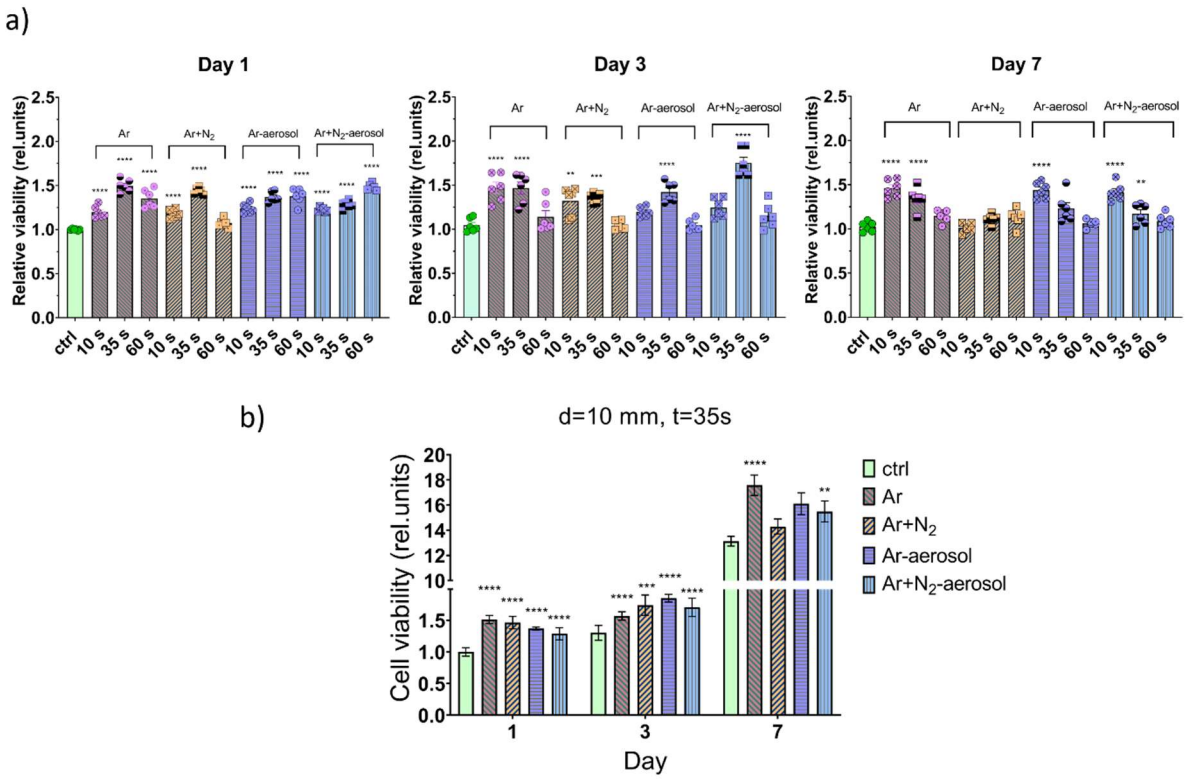

Figure 3. *In vitro* study on the cell viability and proliferation: a) Fibroblast viability of fibroblasts after being treated with plasma relative to the untreated sample using a Presto Blue assay (Day 1, Day 3, and Day 7 after plasma exposure) and b) Viability of plasma-treated fibroblasts after being treated with different plasmas for 35 s relative to the untreated control group of the first day. This representation is favorable for following the exponential growth of the cells during the monitoring days.

In general, for all three examined time points (1, 3, and 7 days after the plasma treatment), the viability values of the plasma-treated fibroblasts are higher than those of the control group (Figure 3(a)). These results indicate that the L929 cell proliferation upon all conducted plasma treatments is considerably higher than in the case of untreated cells. In addition, regardless of the treatment condition, all plasma-treated cells exhibit a higher cell viability (even up to 75% higher (see day 3, treatment with Ar+N_2-aerosol, t=35s)) relative to the untreated control, and hence all applied plasma treatment conditions can be considered non-toxic, which is in accordance with literature[40]. The plasma-induced enhancement of cell proliferation can be attributed to the oxidative stress that the cells experience after exposure to plasma RONS. That is, the cells protect themselves from possible ROS damage through oxidant-induced activation of cellular signaling pathways. Furthermore, these cells respond to mild oxidative stress (10-60 s exposure to plasma) by proliferating through cross-communication between the cellular signaling systems and the cellular redox state[16, 38]. Thus, cells determine their fate, such as cell proliferation, via cross-talk. A previous study reported that ROS from plasma promotes fibroblast growth factor (FGF-2) release, the main mechanism governing plasma-induced cell proliferation[20]. The ROS-responsive behavior of the cells results from the tendency of each cell to adapt to oxidative stress via upregulation of the defense system. This may result in partial/complete protection from damage or overprotection and resistance development[38].

For each of the three different experimental groups under study (10, 35, and 60 s), cell proliferation is similar, as shown in Figure 3(a). However, different cell proliferation behavior within each experimental group is observed during these treatment times, particularly when no aerosol is used in the system. Figure 3(a) indicates that the viability of the Ar and Ar+N_2 plasma-treated fibroblasts on day 1 is the highest (50 % increase relative to the viability of the control) for the experimental groups treated for times of 35–60 s and 10-35s, respectively. Addition of N_2 to Ar plasma results in temporal modification of generated RONS (increase in RNS) and as such

the proliferative effect on fibroblasts might differ (Figure 3(a), Day 1). Cells treated 35 s with Ar/Ar+N_2 plasma exhibited enhanced proliferation as a response to the moderate flux of RONS and the corresponding oxidative stress. However, during the following days (up to day 7), the cell growth rate decreased, probably owing to the adaptation of the cells to the RONS introduced in their environment (see Figure 3(a), day 1, 3 and day 7 for 35 s). Obviously, a longer treatment of 60 s with Ar/Ar+N_2 plasma offering a higher flux of RONS results in poorer cell adaptation and thus a more drastic proliferation decrease in days 3 and 7. The opposite trend is observed for the proliferation of the experimental group treated with the plasma during a shorter time of 10 s. The cells treated with a short exposure to Ar plasma and thus a lower flux of RONS underwent a gradual increase in proliferation and adaption to the RONS environment. The maximal proliferation reached a 50 % increase relative to that of the control on day 7 (see Figure 3 (a), day 7 for 10 s). An established H_2O_2 oxidation model can explain various cell responses as a function of RONS concentration. Namely, adding a low concentration of H_2O_2 (3-15 uM) to mammal cells causes a significant mitogenic response (25-45% growth simulation). Larger concentrations of H_2O_2 (120-150 uM) would cause a temporary growth arrest followed by adaptation. The temporal behavior of cell proliferation during the seven days of monitoring performed in this work can be explained through similar mechanisms inducing cell growth or growth arrest. However, essential to notice is that H_2O_2 is not the only RONS produced by plasma in the cell environment. Therefore, different responses can be induced in 10, 35, and 60 s plasma treatment. Moreover, the post-discharge chemistry may influence the change of RONS concentration and other outcomes than predicted with the H_2O_2 oxidation model. Accordingly, slight difference in cell proliferation behavior between Ar and Ar+N_2 experimental groups rises due to the variation of produced RONS. In addition to the cell proliferation of all experimental groups (Figure 3(a)), cell proliferation after 35s treatments normalized on the untreated control sample of the first day is presented on Figure 3(b). Treatment time 35 s has been chosen as optimal[32] and following experiments on gene expression and cell permeabilization are conducted for this plasma treatment time. Figure 3(b) shows healthy exponential growth of fibroblast cells during the 7 days of culturing after treatments with Ar, Ar+N_2 plasma and their aerosol counterparts.

In addition, to substantiate the trends observed by the Presto Blue assay, cell viability was also visualized using a live/dead assay 1 day, 3 days and 7 days after plasma exposure. Stained fibroblasts on day 1 and day 3 after the Ar plasma and Ar plasma-aerosol treatment are shown in Figure 4. On day 7, the cell morphology observation is rather challenging as a complete cell confluent layer covered the well-plate; accordingly, the fluorescence images corresponding to the last sampling day are only presented in the supplementary information (Figure S1).

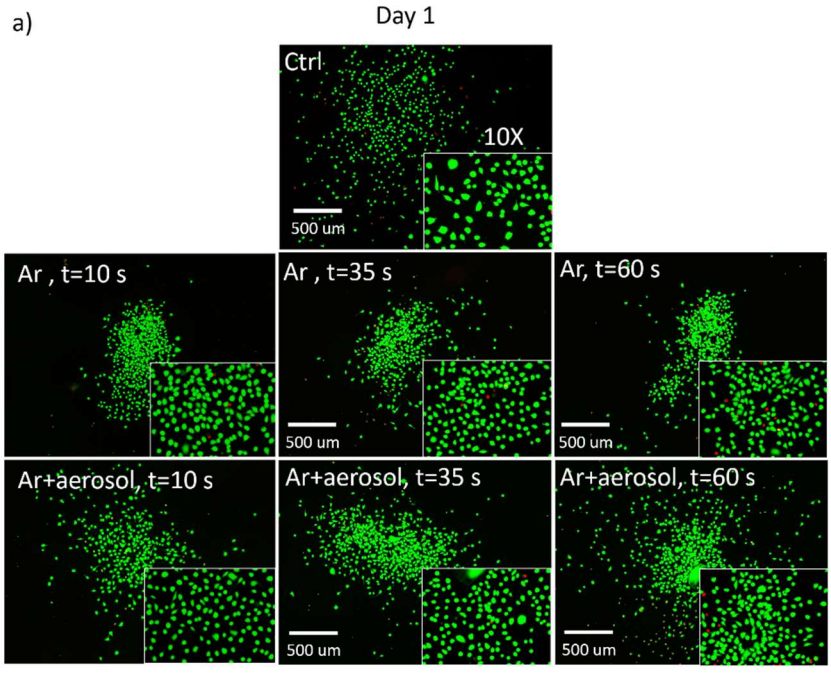

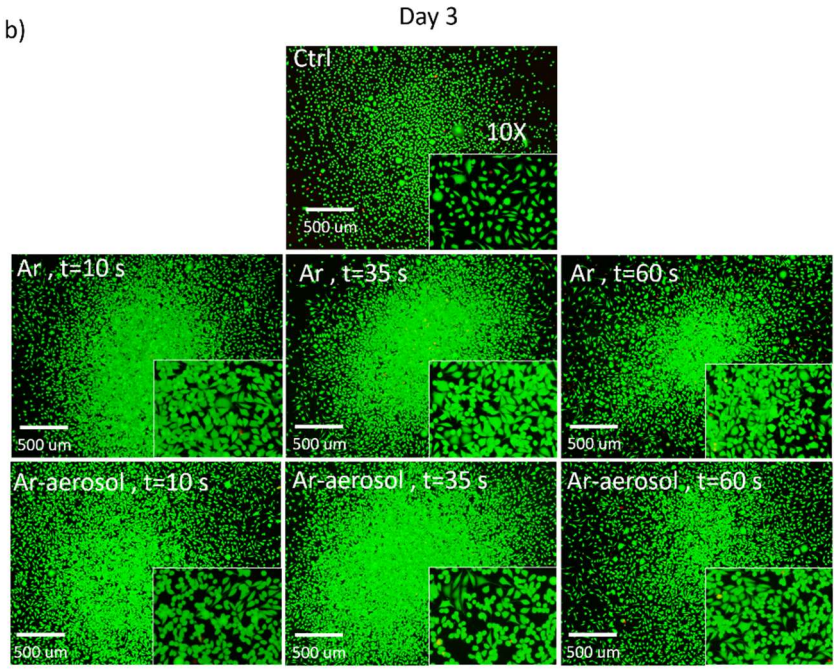

Figure 4. Live (green)/dead (red) staining (magnification 4x and 10x) a) Day 1 : Control; Ar plasma t= 10 s (left), t=35 s (middle) and t=60 s (right); Ar-aerosol plasma t= 10 s (left), t=35 s (middle) and plasma t= 60 s (right). b) Day 3: Control; Ar plasma t= 10 s (left), t=35 s (middle) and t=60 s (right); Ar-aerosol plasma t= 10 s (left), t=35 s (middle) and plasma t= 60 s (right).

Fluorescence staining of fibroblasts reveals a high survival rate of the plasma-treated cells, especially in the case of shorter plasma exposure times (e.g., 10, 35 s, day 3) for all experimental groups. Figure 4 (a) reveals that 1 day after plasma exposure, the untreated cells consist of living cells with a round morphology (~60% of all cells), suggesting poor cell adhesion to the well plate. In contrast, in the case of all plasma-modified fibroblasts, a higher number of living cells can be observed with a more spread-out morphology proving the excellent initial adhesion to the well plate of these cells (more visible on day 3). Although the staining technique presents only qualitative resuts, it has to be mentioned that no essential difference in cell morphology has been noticed between cells treated with Ar and Ar-aerosol plasma. Cell attachment to the substrate and to other cells is mediated by cell-adhesion molecules (CAMs) referred to as integrin and cadherin, respectively. However, CAMs can be easily damaged by overexposure to ROS-induced oxidative stress associated with oxidation of the adhesion proteins located on the exterior of the cell[41]. For all modification conditions, 1 day after plasma exposure, cells' attachment to the middle of each well (similar to the control sample) surface occurs at a similar density. This indicates that the plasma treatments (under all conditions) cause no damage to either cadherin or integrin, and the integrity of the cells is maintained during the treatment. Additionally, 3 days after exposure to plasma, more strongly adhered fibroblasts with a more flattened morphology than that of the untreated cells are observed in the plasma-treated samples (see, for example, Figure 4 (b) Ar-aerosol; t=60 s). This morphology corresponds to the differentiated fibroblasts (myofibroblasts) observed on tissue culture polystyrene plates and may indicate excellent cell differentiation. It must be mentioned that no significant difference in cell morphology has been observed when cells are treated with Ar and Ar+N_2 plasma without and with aerosol, accordingly only images regarding Ar and Ar-aerosol plasma treatment are presented.

3.2. Wound healing study through gene expressions in plasma-treated cells

The standard wound healing model is described through four overlapping phases: hemostasis, inflammation, proliferation, and remodeling[42]. During the hemostasis or coagulation phase, erythrocytes are recruited in the wound bed, while in the inflammation phase, macrophages and neutrophils are recruited to fight infection. The wound healing in the proliferation and remodeling phase is owed to the connective tissue, thus

owed to fibroblast cells. Fibroblast cells migrate towards the injury and adhere to the wound bed, thereby proliferating and repairing the damage. The proliferation phase of a wound is followed by stages including matrix remodeling, differentiation of fibroblasts into myofibroblasts, and healthy scarring without fibrosis[43]. In this context, many proteins are produced and are responsible for the healthy healing of a wound. As mentioned, the role of fibroblasts in the proliferation and remodeling phase is crucial, and it mirrors in their activities such as migration, adhesion, proliferation, differentiation, and secretion of one of the most abundant ECM proteins, collagen. According to literature, skin tissue regeneration utilizing cold plasma is accompanied by regulation of focal adhesion, matrix remodeling, and tissue oxygenation[44]. ROS are crucial for activation (phosphorylation) of the integrin adhesions (FAK, PXNα), alterations of integrin's structural proteins (TLN, VCL) and organization of actin, improved deposition of ECM protein collagen, and the formation of new cell-matrix contacts[44]. As shown in Figure 5, cell-matrix interactions are realized through integrin focal adhesions and syndecans. Both groups of protein receptors are responsible for the migration and adhesion of the cells. Cellular migration follows the process of repetitive esembly and disassembly of new cell-matrix contacts through the mentioned protein groups[44]. The cell surface-adhesion complexes are crucial in signaling pathways and maintaining adhesions to ECM through a series of integrin's proteins, including FAK, PXNα, VCL, and TLN. Other than via integrin's proteins, communication between cell and matrix is also occurring via syndecans (SDC 1,4). Syndecans play an important role in extra- and intracellular signaling cascades as adhesion receptors and grow factor co-receptors. Collagens, the most abundant ECM proteins secreted by cells, also play a vital role in the remodeling stage of the wound healing process[45].

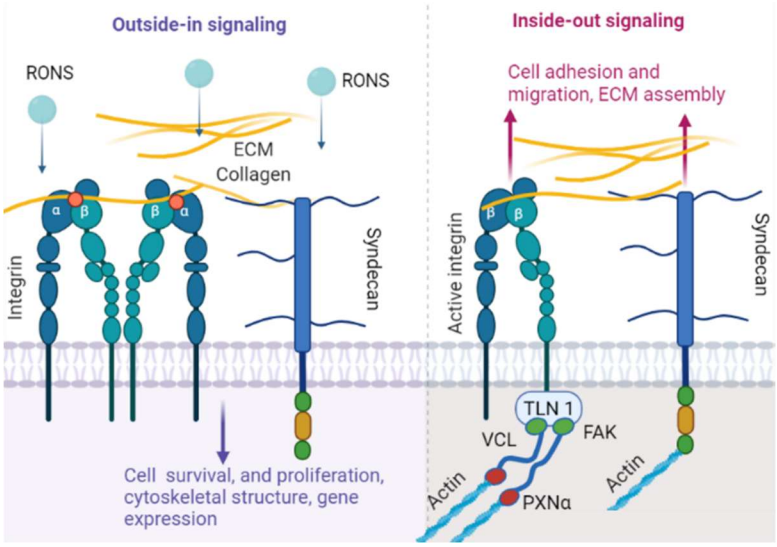

Figure 5. Visualization of cell-matrix communication realized through integrin focal adhesions and syndecans.

3.2.1.Gene expression in plasma-treated fibroblast cells

In this paper, the underlying molecular mechanisms regulating fibroblast adhesion, proliferation, and differentiation upon exposure to plasma-induced RONS are identified by examining the expression levels of surface-adhesion-related markers. In addition, comprehensive information regarding the regulatory influence of RONS, and more specifically RNS, on the wound healing process is gathered. To this end, the plasma-induced cellular responses critical to the wound healing are studied by evaluating the expression levels of genes responsible for cell adhesion and motility (TLN, VCL, PXNα, FAK, SDC1, and SDC4 as transmembrane matrix receptors), cell-matrix communication (COL 1A1 and IV), proliferation (Ki-67), and differentiation (α-SMA). Experiments have only been performed using a plasma treatment time of 35 s, which is considered to be an optimal treatment time. Cells treated for 35 s with the plasma jet experienced the highest proliferation rate during the first three days of monitoring. Moreover, the 35 s treatment with plasma and plasma-aerosol is validated to be safe when treating bio-objects[32].

Gene expressions were assessed 6 h, 24 h, and 48 h after the plasma treatment with Ar, Ar+N_2, Ar-aerosol, and Ar+N_2-aerosol. The gene expressions normalized to the untreated control are presented in the form

of a heat map (see Figure 6 (a, b) for 6 h post plasma exposure and 48 h post plasma exposure, respectively). As an example, quantitative PCR results for the three-time points 6, 24, and 48 h are presented for the focal adhesion vinculin VCL and the most abundant ECM protein collagen I COL 1A1 in Figure 6 (c, d). Separate graphs obtained for the three-time points under study of all measured genes are also shown in the supplementary information (S2).

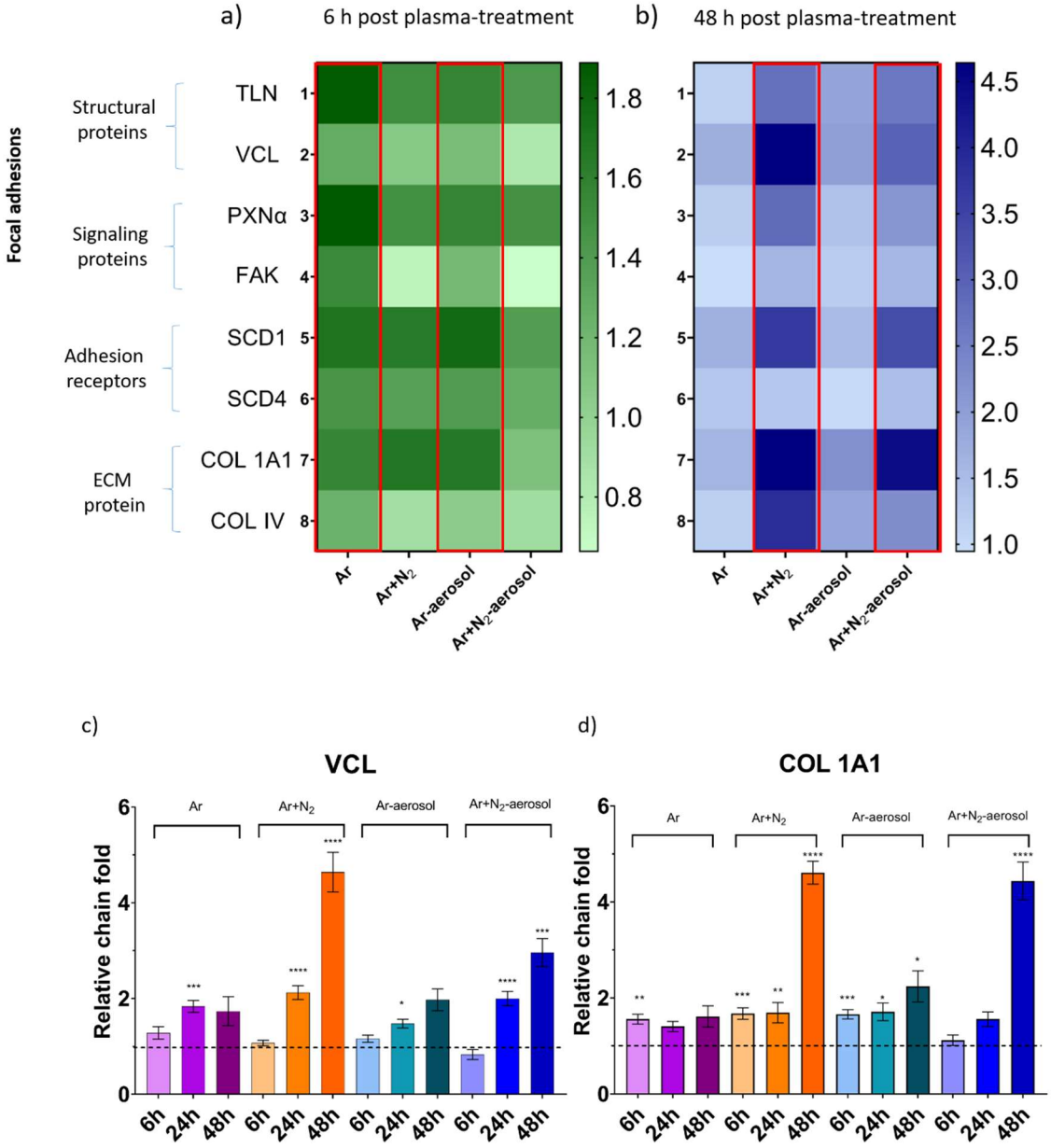

Figure 6. Gene expression analysis; relative chain fold on the expression of talin (TLN), vinculin (VCL, below, left), paxillin (PXNα), focal adhesion kinase (FAK), syndecan (SCD) 1 & 4, and collagens (COL 1A1, below, right) & COL IV a) 6 h after plasma treatment and b) 48 h after plasma treatment. Quantitative gene expression results have been normalized to GAPDH (glyceraldehyde-3-phosphate dehydrogenase), and results presented in the heat map have been normalized to the untreated control sample (dashed line, relative chain fold of value 1).

Compared to the untreated cells, a higher upregulation of cell adhesion/migration marker expression is observed for almost all plasma-treated cells after 6 h and 48 h (see Figure 6). Various differential expression patterns and functions of individual integrins are observed in the L929 cells indicating the high dependency of cell fate on the plasma conditions (either carrier gas or with/without aerosol) and the time after plasma exposure. More

specifically, 6 h after plasma treatment, the expression level (for all markers) is more pronounced after Ar and Ar-aerosol plasma treatment (Figure 6 (a), red boxes) than after the treatment with $Ar+N_2$ and $Ar+N_2$-aerosol plasma. In fact, in the gas plasma fed by Ar, ROS and UV radiation are dominant reactants. Most of the ROS present in the plasma are short-living species (OH, O, $^1O_2$, O_3[31]) followed by long-living species such as H_2O_2 (10 µM). However, the addition of only 0.05 % of N_2 to the Ar plasma yields the highest gene upregulation measured 48 h after plasma treatment (see Figure 6 (b), red boxes). The addition of N_2 to the Ar gas results in a boosted NO production and, accordingly, a boost in downstream long-living products such as NO_2^- and NO_3^- (see Section 2.1). Namely, the plasma-generated ROS (in early cell culture time, 6 h) and RONS (in late cell culture time, 48 h) induce an upregulation of vinculin with the relative folds 1.75 and 4.65 and collagen I with the relative folds 1.55 and 4.6 (Ar/Ar-aerosol plasma 6 h, $Ar+N_2$/ $Ar+N_2$-aerosol plasma 48 h). More information on the chemistry of the RNS species is given in the supplementary information (SI).

The maximal expression of the focal adhesions genes, syndecans, and collagens is reached 48 h after treatment with $Ar+N_2$ plasma. This can be ascribed to the higher concentration of long-living ions NO_2^- and NO_3^-. As follows, the highest upregulation of the measured genes occurs 48 h after $Ar+N_2$ and $Ar+N_2$-aerosol plasma treatment due to 1) total consumption of nitrates and nitrites after 48 h (SEq 1-9), or 2) post-discharge activity of the slightly acidic cell medium and prolonged generation of NO_x ions species in thse conditions (SEq 10-12).

3.2.2. Cell-matrix integrin-based adhesion proteins and ECM proteins

A previous study reported that upregulations in structural proteins (vinculin and talin) result in improvement in intracellular signaling and intercellular connections, which are essential for wound closure[44]. Moreover, the study hypothesizes that vinculin is a plasma-regulated switch in the dynamics of focal adhesions and a useful target for optimizing the care of non-healing wounds. Indeed, ECM proteins such as collagens and integrins perceive extracellular signals from plasma-induced active species through activation of vinculin and talin, associated with actin and integrin stimulations. Such changes are then passed to signaling proteins by changing protein kinase phosphorylation levels (e.g., focal adhesion kinase) as a decisive factor in cellular responses. These responses improve cell migration toward the wound site, boosting re-epithelialization and further matrix deposition. Our results in this work confirm that levels of focal adhesions (TLN, VCL, PXNα, FAK), syndecans (SCD 1,4), and collagens (COL 1A1, IV) increase upon alternation in cellular architectures under oxidative stress (Figure 6). All measured genes experience the same trends with gas composition and post-treatment time, as shown in Figure 6 (a, b).

The highest expression of focal adhesions PXNα, FAK, and TLN is observed 6 h after treatment in case of treatment with Ar and Ar-aerosol plasma, resulting in relative folds 1.5-2 (Figure S2 (a, b, e)). On the other hand, focal adhesions reach a maximal expression only after 48 h when cells are treated with Ar/N_2 and Ar/N_2-aerosol plasma. 48 h after treatment with $Ar+N_2$ and $Ar+N_2$-aerosol plasma, the expression of focal adhesions reaches much higher relative folds for VCL compared to the Ar plasma (2.5 to 4.6), as shown in Figure 6 (c). The same trend holds for syndecan 1 (SDC 1). The gene expression level (relative fold 2) during a short post-treatment time (6 h) using Ar/Ar-aerosol carrier gas is doubled after treatment with $Ar+N_2$/ $Ar+N_2$-aerosol plasma during a long post-treatment time (48 h) (relative fold 3.7 and 3.4 respectively). This suggests that Ar-plasma-induced ROS (in short post-treatment time) and $Ar+N_2$ plasma-induced RNS (in long post-treatment-time) tune extracellular signal transfer across the cell surface to the cytoskeleton. Such a transfer would influence the activation of various intracellular signaling cascades through stimulation of SDCs. Opposite to highly expressed SDC1, expression of syndecan 4 (SDC 4) for all experimental groups is measured to be slightly above the untreated control (relative fold maximal 1.5 in case of $Ar+N_2$-aerosol plasma). The aforementioned higher expression level of SDC 1, 4 allows direct contact of the cells with ECM (see Figure 5). Moreover, syndecans (SDC 1, 4) have an important role when clustering with other proteins such as HER2, α6β4 integrin, and αvβ3,5, which stimulate cell invasion, survival, and angiogenesis. Similar to our results for L929, Schmidt et al. [44] also found upregulation of both growth factor co-receptors (SDC 1/4) during 24 h after Ar plasma-assisted treatments of primary dermal fibroblasts. This corresponded to increased cell migration and growth factor uptake.

A previous study reported that fibroblast proliferation is associated with a collagen-rich ECM reconstitution[44]. Hence, in this study, we also screened the secretion of collagen I and IV post plasma treatment (Figure 6 (a, b, d) and Figure S2 (f)). Indeed, fibroblast survival increases in response to external stimulation (induced by plasma modification) from the microenvironment, and this increase is manifested by the secretion of ECM components (e.g., collagens). Compared with the expression level observed for untreated cells, the expression level of collagens COL 1A1 and COL IV is significantly higher for plasma-treated fibroblasts. Precisely, after a short post-treatment time (6 h) for all plasma systems under study, COL 1A1 and COL IV are upregulated up to 2 relative folds, while after a longer post-treatment time (48 h) and treatment with Ar+N_2 and Ar+N_2-aerosol plasma, the upregulation of this ECM collagens increases with 100 % thus above 4 relative fold. Gene expressions of focal adhesions, syndecans, and collagens reach a maximum value at 48 h post-treatment time when the treatment was performed using an Ar+N_2 and Ar+N_2-aerosol plasma. This trend can be attributed to the post-discharge chemistry and the generation of long-living species NO_2^- and NO_3^- in the cell medium by plasma[46]. Important to mention is the variety in the spectra of generated species by Ar, Ar+N_2 plasma, and their aerosol counterparts. As demonstrated in our previous studies[31-32] and highlighted in Section 2.1., short-living ROS dominate the Ar plasma, while adding N_2 to the Ar feeding gas yields the generation of long-living species such as NO_2^- and NO_3^-. Accordingly, adding 0.05% of N_2 to the Ar plasma results in a higher concentration and variety of long-living RONS, which seem to play a crucial role in the activation of wound-healing genes.

3.2.3. Cell proliferation and differentiation markers

Upon plasma exposure, most of the cells are viable at all three-time points (day 1, 3, 7); however, the proliferation rate increases more slowly in the early stage after plasma treatment (between days 1 and 3) than in the long cell culture (between day 3 and 7) (Figure 3(b)). Messenger ribonucleic acid (mRNA) transcripts of the marker associated with proliferation Ki-67 is therefore screened for three different time points (6, 24, and 48 h post-plasma treatment time). The corresponding results (see Figure 7 (a)) reveal that Ar-plasma-induced ROS (with/without aerosol) leads to a downregulation of Ki-67 from 6 h to 48 h. This indicates that the impact of ROS species on the proliferation rate of L929 is less favorable in the initial two days after the plasma treatment than under other plasma conditions. In contrast, Ar+N_2 plasma-induced RONS (with/without aerosol) result in upregulation of the proliferation-related marker, thereby revealing numerous proliferating L929 cells during the first two days. These results suggest that the alternation in proliferation after 48 h was induced by incorporating long-living nitrogen species rather than by incorporating short-living oxygen species.

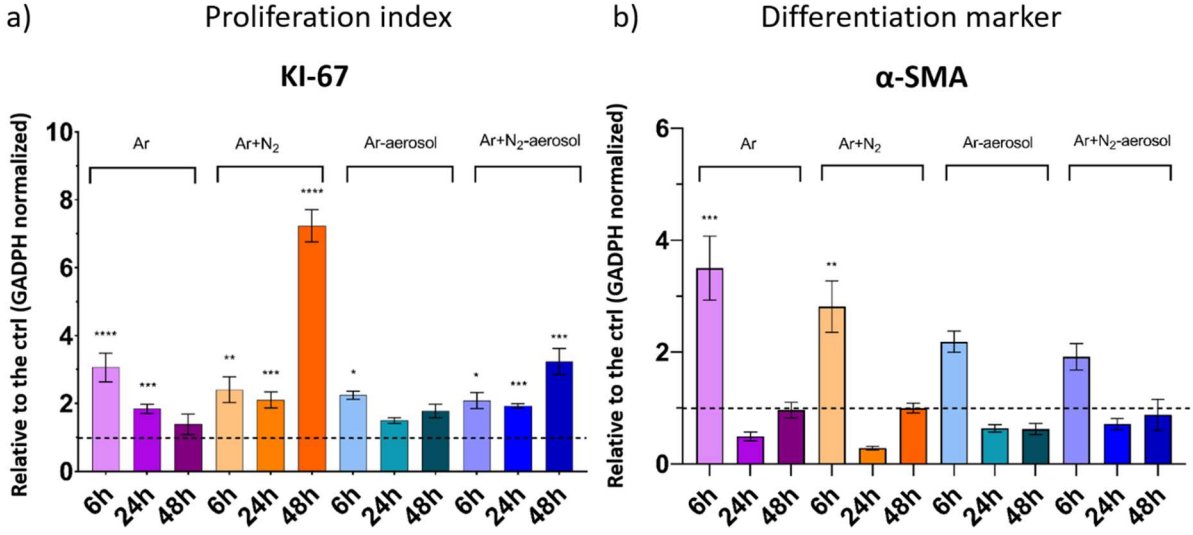

Figure 7. a) Gene expression level of a proliferative index (Ki-67) and b) gene expression level of the differentiation marker α-smooth muscle actin (α-SMA) indicating fibroblast differentiation towards myofibroblasts, 6 h, 24 h, and 48 h after the plasma treatments, presented relative to the untreated control samples (1)

As previously explained, the differentiation of fibroblasts into myofibroblasts is considered the last step in the proliferation and remodeling stages of the healthy wound healing process. Assessing the influence of each plasma treatment on the fibroblast-to-myofibroblast transition stage is therefore essential. To this end, the expression of the myofibroblasts-related marker α-smooth muscle actin (α-SMA) is examined. Unlike focal adhesions which are maximally upregulated 48 h after plasma treatment, the α-SMA differentiation marker is highly upregulated in the first 6 h after the plasma treatments with/without aerosol (Figure 7(b)). In addition to this, important to notice is that upregulation of the differentiation marker is the highest in the case of treatment with Ar plasma, which is dominated by mainly short-living ROS. The α-SMA expression level in the Ar plasma-treated cells 6 hours after exposure is almost four times higher than that of the untreated cells. Furthermore, in treatments with other carrying gases including Ar+N_2 (relative fold 3), Ar-aerosol (relative fold 2.2), and Ar+N_2-aerosol (relative fold 2) plasma, the concentration of ROS is lower. This indicates that the differentiation of fibroblasts into myofibroblasts is mainly induced by both short- and long-living ROS, although the effect of the former on the differentiation stage is more prominent than that of the latter. The improvement in fibroblast differentiation is attributed to the stimuli effect of plasma-induced ROS in GF secretion. Previous studies have reported that fibroblasts release TGF, an essential factor for differentiation, upon exposure to an oxidative stress[20, 47]. In conventional therapies, TGFs are added as a therapeutic to improve the proliferation of cells[7, 48], which is often achieved by adding a high concentration of TGF to culture media. This high concentration has negative effects such as cell toxicity (in some cases), quick cell saturation, and waste of expensive GFs. However, our results revealed the excellent effect of plasma modification on the fibroblast-to-myofibroblast transition stage (in the absence of wound-healing related GF), indicating the outstanding potential of plasma exposure in wound healing applications. Plasma exposure can trigger fibroblast responses (namely focal adhesions, proliferation, and differentiation) associated with healthy wound healing. Plasma mechanisms of fibroblast activation lay in the rich initiated RONS chemistry. Although cell responses upon plasma treatment are often assigned to ROS, this study confirms the mutual importance of RNS, specifically NO downstream products such as NO_2^- and NO_3^-.

As this work focuses on an *in vitro* study of plasma-assisted wound healing advanced by drug delivery, after the proliferative character of short plasma/plasma-aerosol treatment has been confirmed above, the effect on cell permeabilization can be be tested in the following. This step is important when studying localized drug delivery using a plasma/plasma-aerosol system.

3.3. Plasma-aerosol advanced wound healing *in vitro*: Cell permeabilization and drug introduction

As previously shown, short plasma treatments (10-35 s) can stimulate cell proliferation and differentiation 7 days after plasma treatment. In this study, an additional step is also performed in an effort to combine the positive effect of plasma on cell proliferation and differentiation with induced cell permeabilization, followed by drug introduction. Accordingly, fluorescently labeled (FITC) dextran has been used as a model drug carrier[37, 49]. Dextrans are non-toxic biopolymers consisting of a few D-glucose molecules joined in long chains of varying lengths. The average molecular weight of dextran plays a key role in determining the size of the biopolymer molecules in an aqueous solution. In this work, the permeabilization of fibroblasts upon plasma treatment is studied using dextrans with molecular weights of 4, 10, 40, and 70 kDa and corresponding hydrodynamic radii of approximately 1.0, 1.9, 4.8, and 6.5 nm. Dextrans can be labeled with a green fluorescence protein (FITC), and their fluorescence intensity can be easily detected once FITC is covalently bound to the targeted cell[50]. Dextrans are used in pharmacology and medicine (microinjection[51], ultrasound cavitation[52], and electrophoresis[53]) to trace drug delivery as these molecules are unable to freely penetrate the cells. To this end, dextrans are perfect candidates for evaluating permeabilization upon plasma treatment and transcellular drug delivery. Plasma delivery of dextran to fibroblast cells has been conducted using Ar plasma, Ar+N_2 plasma, and their aerosol counterparts Ar/ Ar+N_2 plasma-aerosol. Cells were exposed for 35 s to the plasma at a distance of 10 mm from the effluent. Full plate imaging via permeable cell fluorescence for the smallest dextran molecule is shown in Figure 8 (a). As shown in the figure, dextran is delivered locally in Ar plasma-treated cells only, and the untreated cells remain unstained. As the localized delivery of dextran to fibroblasts with Ar and Ar+N_2 plasmas is

almost identical, images corresponding to Ar+N_2 plasma permeabilization of cells are only provided in the SI. However, the localized delivery to permeabilized cells differs significantly between cases employing gas plasmas and aerosol-assisted plasmas, as can be seen in Figure 8 (a). Simulation of mechanisms how plasma and plasma-aerosol cause cell permeabilization is shown in Figure 8 (b, c). COMSOL MultiPhysics model for Ar hot gas with and without microdroplets has been developed and explained in detail in our prievious work[32]. Accordingly, in this work the model has been used in order to visualize and understand different mechanisms of cell permeabilization by Ar/Ar+N_2 plasma (Figure 8(b)) and Ar/Ar+N_2 (Figure 8(c)) plasma in combination with aerosol.

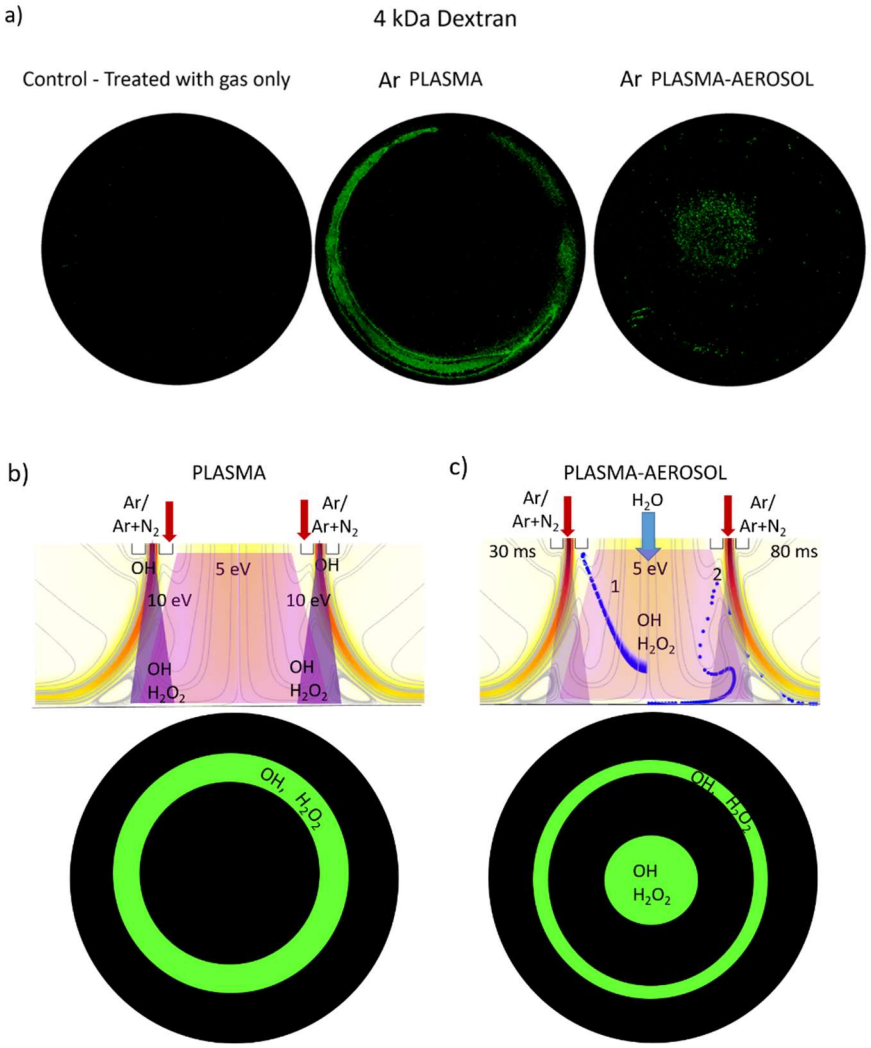

Figure 8. a) 4 kDa Dextran introduction into untreated, Ar and Ar/aerosol plasma-induced permeable cells. COMSOL MultiPhysics simulations of localized cell permeabilization and dextran delivery via b) Ar plasma and c) Ar plasma-aerosol treatment.

In the case of the Ar plasma-treated fibroblasts, localized cell permeabilization and the introduction of dextran occur in the outer annular region of the plasma. However, upon plasma-aerosol exposure, cell permeabilization and dextran introduction occur in the area corresponding to the aerosol injection region, as can be seen in Figure 8 (a). Previous research on cell permeabilization using a He RF plasma jet[37] proposed two governing mechanisms for cell-membrane poration: cell charging induced by heavy ions[54] and lipid peroxidation of the membrane by OH radicals and H_2O_2[41]. The first mechanism plays an essential role in direct plasma treatments, where treated cells are directly exposed to the heavy ions from the plasma[55]. However, in a plasma jet, where cells are indirectly exposed to plasma, ions and electrons recombine shortly after exiting the nozzle

and are therefore considered non-essential in the permeabilization of cells. However, OH radicals and H_2O_2 species are abundantly created in plasma jets in contact with water[56] and may therefore play a major role in transient pore creation via lipid peroxidation of the plasma-treated cells.

The different plasma localized dextran delivery patterns with and without the use of aerosol can be explained by changes in plasma chemistry once aerosol droplets are introduced into plasma effluent. During the treatment with Ar (or Ar+N_2 plasma), OH is generated as a dissociation product of water impurities in the feeding gas (plasma), ambient air (close effluent), and the aqueous layer covering the cells (UV radiation). The dominant reactions occurring in the Ar jet operating under humid conditions are presented in Equations (1-3)[34]. Moreover, considering the intense UV radiation from Ar excimers Ar_2^* and atomic oxygen OI (E_{hv}~10 eV) in the plasma, the contribution of water photodissociation must not be neglected (E_{diss}=4.4 eV for O-H bond) (Eq 4).

$$Ar_2^+ + H_2O \rightarrow 2Ar + H_2O^+ \rightarrow H_2O^+ + e^- \rightarrow OH + H \quad \text{Eq 1.}$$

$$Ar_2^+ + H_2O \rightarrow OH + ArH^+ + Ar \quad \text{Eq 2.}$$

$$Ar(4s[3p_2]) + H_2O \rightarrow Ar + OH + H \quad \text{Eq 3.}$$

$$H_2O \xrightarrow{\frac{h\nu}{5\ eV}} OH + H \quad \text{Eq 4.}$$

In the far effluent, OH radicals tend to recombine in three-body collisions, forming long-living H_2O_2. Indeed, in the presence of Ar, N_2, O_2, H_2, H_2O, and O_3[34], OH radicals dimerize in H_2O_2 (Eq 5).

$$OH + OH + M \rightarrow H_2O_2 + M \quad \text{Eq 5.}$$

The introduction of aerosols in the plasma effluent spatially translates the plasma-initiated chemistry from only the outer plasma ring region to both the outer plasma ring and the inner effluent region. Namely, due to the larger interface between the plasma jet and aerosol droplets compared to the plasma jet and the liquid bulk in the well plate, the plasma jet favors interaction with aerosol droplets over an aqueous target[31, 57]. Accordingly, the favorable interaction with the aerosol modifies the spatial distribution of plasma-generated species as described in our previous publication[31-32]. Considering the pattern of localized cell permeabilization by the plasma-aerosol system, it can be seen that drug-delivering molecules, namely OH and H_2O_2, also originate from the aerosol. The interaction of the plasma jet with aerosol results in OH radicals and H_2O_2 generation, which are shielded and safely transferred[58] to the cells covered by the dextran layer (see Figure 8 (b)). As this interaction mainly occurs in the plasma-free region, the interaction of water droplets and RONS and UV radiation is limited, further resulting in lower OH and H_2O_2 concentrations, in comparison with the effect of plasma solely. Although most of the cell permeabilization in plasma-aerosol treatments occurs using activated aerosols, a weaker and not always obvious permeabilization also partially occurs in the outer plasma ring region (see Figure 8 (c)). Possibly, partial diffusion of micro-droplets or water vapor towards the region of the outer plasma ring effluent (Figure 8 (c)) can impact the formation of OH radicals by quenching precursors, e.g., electrons and Ar metastables. Other mechanisms can be assigned to the complete photolysis of water vapor in the plasma effluent ring region by high-energy UV photons emitted from the inter-electrode region and further quenching of atomic oxygen, as shown in equation Eq 4-6:

$$H_2O \xrightarrow{\frac{h\nu}{8.8\ eV}} 2H + O \quad \text{Eq 6.}$$

Different sizes of dextran are investigated for plasma-induced cell permeability and transient membrane poration. Cell permeabilization by means of Ar plasma and Ar plasma coupled with aerosol is presented in Figure 9. Cell permeabilization by means of Ar plasma for four different size dextrans is presented as a full plasma ring;

for this purpose, the plasma-treated area is cropped in quarters. Dextran of the lowest molecular weight is the most efficiently incorporated into the permeabilized cells, as shown in Figure 9 (a). Accordingly, the fluorescence of 4 kDa dextran labeled with FITC is detected with the highest intensity. During plasma treatment, the smallest nanopores (~1 nm) are created along the complete outer plasma ring (d~22 mm). Larger pores (1.9–6.5 nm) corresponding to the introduction of larger dextran only occur along 50 % in case of 10 kDa and 25% of the plasma ring length in case of 40 and 70 kDa dextran. This may have resulted from the slight decentralization of the electrodes and the local variation in OH and H_2O_2 concentrations along the plasma ring. Localized dextran delivery in permeabilized cells utilizing plasma combined with aerosol did not essentially differ for 4, 10, 40, and 70 kDa molecules, as shown in Figure 9(b). The delivery of dextran appeared dominantly in the aerosol region, while for the lighter molecules 4 and 10 kDa (d≈1.0, 1.9 nm) weak delivery in the region of the plasma ring could be noticed. However, in case of the heaviest dextran (70 kDa, d≈6.5 nm) the area corresponding to the delivered dextran is the smallest. Although it is expected for lighter molecules to penetrate permeabilized cells in the higher concentration then heavier molecules, no drastic difference of fluorescence intensity has been measured during imaging. It has to be mentioned here that the used imaging technique is purely qualitative and for more information about concentration of delivered dextrans other quantitative analysis would have to be performed.

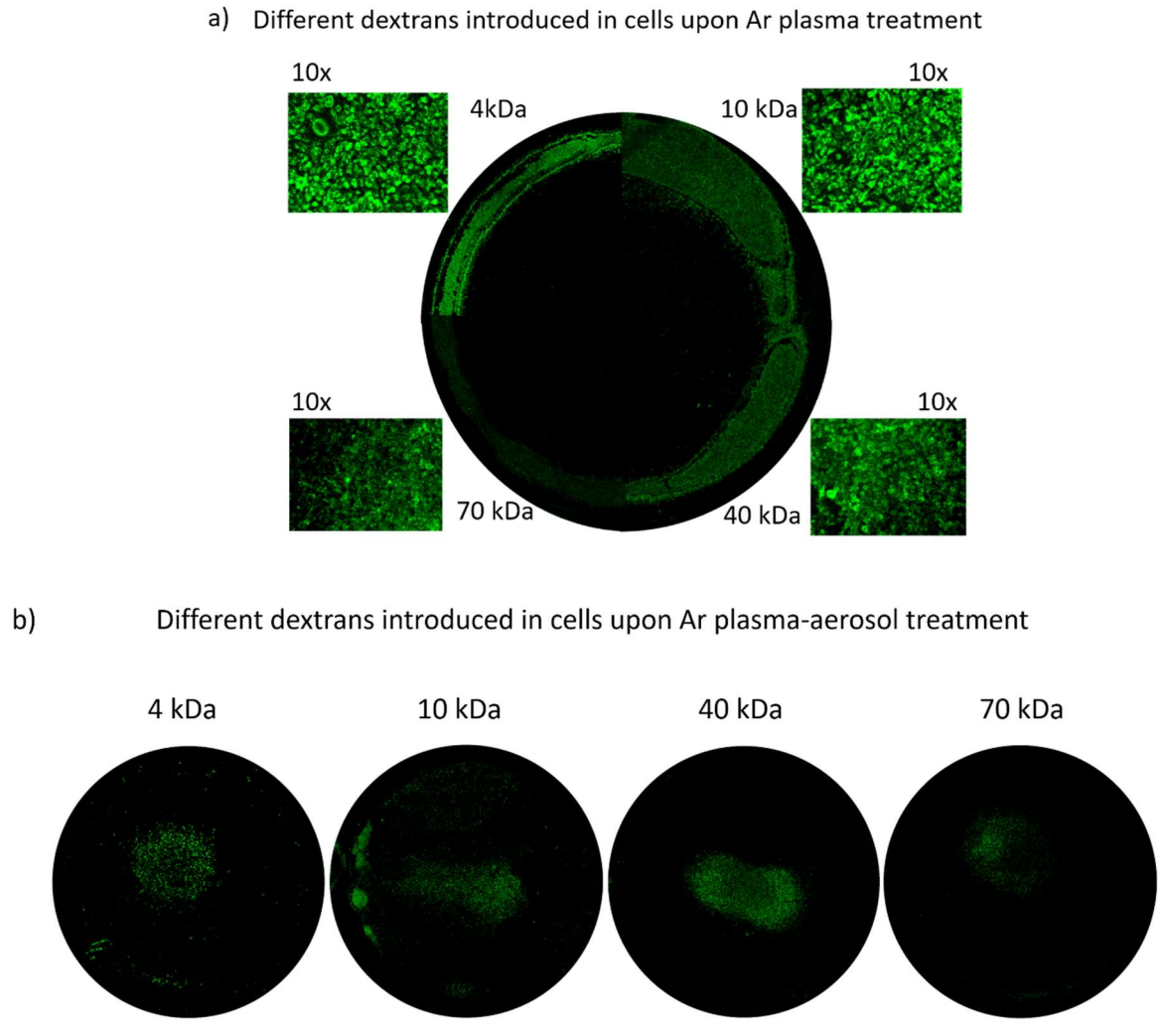

Figure 9. a) Ar plasma and b) Ar plasma-aerosol induced localized cell permeabilization and introduction of 4, 10, 40, and 70 kDa dextrans. Fluorescence of delivered dextran-FITC is imaged on the whole treated area while insets present 4x magnification. For a better representation, the brightness of all images was increased by 50%.

A similar study on HeLa cell permeabilization by a He RF plasma jet[37] has also reported the size limitation of molecules that can be introduced during the plasma permeabilization process. In this study, pores smaller than 6.5 nm were created, and transfection of 6 nm plasmid DNA with an efficiency of 30 % was achieved. On the other hand, the pores created using this He jet were limited to introducing the smallest dextrans (4 and 10 kDa[37]). In another study, a 20% efficiency gene transfection of plasmid DNA (4.7 kbp≈10-13 nm[59]) was realized with a 1-3 s plasma treatment using an air AC plasma jet (40 kHz)[60]. This study reported the creation of transient pores in different cell lines (HeLa, epithelial, connective tissue HT-1080, breast tissue MCF7, and bone marrow cells SH-SY5Y), with a low cell mortality (2%) after plasma transfection. The use of cold plasma for gene transfection thus provides a relatively high efficiency and a low cell mortality, compared with that of electroporation (transfection efficiency ~38% and cell mortality ~11%). In addition, plasma offers a simple procedure and no special reagents are needed.

To conclude, this study has thus focused on localized drug delivery and its manipulation through spatial changes in the concentrations of OH and H_2O_2, which are the drug delivery molecules. Although the used plasma jet system shows interesting features for successful drug delivery, its application is limited when cells are only covered by a small amount of liquid. On the other hand, as shown before and also shown in this work, the same plasma jet system, but coupled with aerosol, offers a good alternative when treating cells and tissues in a limited liquid environment[32]. The introduction of microdroplets into the plasma jet changes the spatial chemistry of the drug delivery molecules and localizes cell permeabilization and drug delivery in the region of the activated aerosol. Consequently, the innovative plasma-aerosol system thus opens up new possibilities and moves existing boundaries of cold plasma applications in medicine.

4. Conclusions

In this study, the potential of an atmospheric pressure plasma-aerosol system in wound healing has been evaluated *in vitro*. Emphasis was made on the possible joint effect of plasma in promoting cell proliferation and permeabilization for drug introduction and enhanced wound healing. The proliferative and permeable effects of Ar and Ar+N_2 plasmas as well as their aerosol equivalents were demonstrated on fibroblast cells (L929). The results revealed that short plasma treatments (t<60 s) have a non-cytotoxic effect on fibroblast cells while promoting their proliferation (increase of 10–40 %). Plasma triggers molecular responses in treated cells and improves cell adhesion, signaling, proliferation, and differentiation. This was demonstrated by studying the expression of genes essential in wound healing. Upregulation of genes such as focal adhesions, syndecans, and collagens is triggered mainly by long-living RNS NO_2^- and NO_3^-. On the other hand, plasma-assisted differentiation of fibroblasts into myofibroblasts, crucial in the last stage of wound healing and healthy scarring, is mainly triggered by ROS.

Moreover, aspects of plasma-driven wound healing enhanced by drug delivery *in vitro* were discussed in this work. Dextran delivery to the plasma-treated cells was realized through cell membrane lipid peroxidation by OH radicals and H_2O_2. Two patterns of dextran delivery were observed, associated with a differently localized cell permeabilization upon plasma and plasma-aerosol treatment. The results revealed that the introduction of aerosol into the plasma effluent changed the spatial distribution of OH and H_2O_2 and accordingly, the local introduction of dextran was changed. This high control over the delivery region can be of great importance in different fiels including localized chemical activation and localized coating deposition. In addition, aerosol introduction into the plasma effluent favored interactions with the aerosol and transferred the occurring plasma chemistry to the aerosol region. This feature can be very interesting for *in situ* plasma modification of biomolecules and their local delivery to a target.

5. Acknowledgements

This study was performed as a collaboration between Ghent University and KU Leuven and was supported by the FWO project “Plasma-skin interactions: from wound treatment to topical introduction of molecules”, number G084917N.

References

1. Singer, A. J.; Clark, R. A., Cutaneous wound healing. *New England journal of medicine* **1999,** *341* (10), 738-746.
2. Vaughan, M. B.; Howard, E. W.; Tomasek, J. J., Transforming growth factor-β1 promotes the morphological and functional differentiation of the myofibroblast. *Experimental cell research* **2000,** *257* (1), 180-189.
3. Smet, S.; Probst, S.; Holloway, S.; Fourie, A.; Beele, H.; Beeckman, D., The measurement properties of assessment tools for chronic wounds: a systematic review. *International Journal of Nursing Studies* **2021**, 103998.
4. Kessler, L.; Bilbault, P.; ORTega, F.; Grasso, C.; Passemard, R.; Stephan, D.; Pinget, M.; Schneider, F., Hyperbaric oxygenation accelerates the healing rate of nonischemic chronic diabetic foot ulcers: a prospective randomized study. *Diabetes care* **2003,** *26* (8), 2378-2382.
5. Moffett, J.; Griffin, N. E.; Ritz, M. C.; George, F. R., Pulsed radio frequency energy field treatment of cells in culture results in increased expression of genes involved in the inflammation phase of lower extremity diabetic wound healing. *The Journal of Diabetic Foot Complications* **2010,** *2* (3), 57-64.
6. Eaglstein, W. H.; Falanga, V., Tissue engineering and the development of Apligraf®, a human skin equivalent. *Clinical therapeutics* **1997,** *19* (5), 894-905.
7. Kiwanuka, E.; Junker, J.; Eriksson, E., Harnessing growth factors to influence wound healing. *Clinics in plastic surgery* **2012,** *39* (3), 239-248.
8. Frykberg, R. G.; Banks, J., Challenges in the treatment of chronic wounds. *Advances in wound care* **2015,** *4* (9), 560-582.
9. Sen, C. K., The general case for redox control of wound repair. *Wound repair and regeneration* **2003,** *11* (6), 431-438.
10. Sen, C. K.; Khanna, S.; Babior, B. M.; Hunt, T. K.; Ellison, E. C.; Roy, S., Oxidant-induced vascular endothelial growth factor expression in human keratinocytes and cutaneous wound healing. *Journal of Biological Chemistry* **2002,** *277* (36), 33284-33290.
11. Sen, C. K., Wound healing essentials: let there be oxygen. *Wound repair and regeneration* **2009,** *17* (1), 1-18.
12. Fridman, G.; Friedman, G.; Gutsol, A.; Shekhter, A. B.; Vasilets, V. N.; Fridman, A., Applied plasma medicine. *Plasma processes and polymers* **2008,** *5* (6), 503-533.
13. Bekeschus, S.; von Woedtke, T.; Emmert, S.; Schmidt, A., Medical gas plasma-stimulated wound healing: Evidence and mechanisms. *Redox Biology* **2021**, 102116.
14. Privat-Maldonado, A.; Schmidt, A.; Lin, A.; Weltmann, K.-D.; Wende, K.; Bogaerts, A.; Bekeschus, S., ROS from physical plasmas: Redox chemistry for biomedical therapy. *Oxidative Medicine and Cellular Longevity* **2019,** *2019*.
15. Kalghatgi, S.; Friedman, G.; Fridman, A.; Clyne, A. M., Endothelial cell proliferation is enhanced by low dose non-thermal plasma through fibroblast growth factor-2 release. *Annals of biomedical engineering* **2010,** *38* (3), 748-757.
16. Kamata, H.; Hirata, H., Redox regulation of cellular signalling. *Cellular signalling* **1999,** *11* (1), 1-14.
17. Fridman, G.; Peddinghaus, M.; Fridman, A.; Balasubramanian, M.; Gutsol, A.; Friedman, G. In *Use of non-thermal atmospheric pressure plasma discharge for coagulation and sterilization of surface wounds*, 32nd IEEE International Conference on Plasma Science, 2005; p 257.
18. Nasir, N. M.; Lee, B.; Yap, S. S.; Thong, K.; Yap, S. L., Cold plasma inactivation of chronic wound bacteria. *Archives of biochemistry and biophysics* **2016,** *605*, 76-85.
19. Laroussi, M., Low temperature plasma-based sterilization: overview and state-of-the-art. *Plasma Process. Polym.* **2005,** *2* (5), 391-400.

20. Kalghatgi, S. U.; Fridman, A.; Friedman, G.; Clyne, A. M. In *Cell proliferation following non-thermal plasma is related to reactive oxygen species induced fibroblast growth factor-2 release*, 2009 Annual International Conference of the IEEE Engineering in Medicine and Biology Society, IEEE: 2009; pp 6030-6033.
21. Shi, X.-m.; Xu, G.-m.; Zhang, G.-j.; Liu, J.-r.; Wu, Y.-m.; Gao, L.-g.; Yang, Y.; Chang, Z.-s.; Yao, C.-w., Low-temperature plasma promotes fibroblast proliferation in wound healing by ROS-activated NF-κB signaling pathway. *Current medical science* **2018,** *38* (1), 107-114.
22. Park, J.; Lee, H.; Lee, H. J.; Kim, G. C.; Kim, S.-S.; Han, S.; Song, K., Non-thermal atmospheric pressure plasma is an excellent tool to activate proliferation in various mesoderm-derived human adult stem cells. *Free Radical Biology and Medicine* **2019,** *134*, 374-384.
23. Laroussi, M., The Resistive Barrier Discharge: A Brief Review of the Device and Its Biomedical Applications. *Plasma* **2021,** *4* (1), 75-80.
24. Breathnach, R.; McDonnell, K. A.; Chebbi, A.; Callanan, J. J.; Dowling, D. P., Evaluation of the effectiveness of kINPen Med plasma jet and bioactive agent therapy in a rat model of wound healing. *Biointerphases* **2018,** *13* (5), 051002.
25. Naik, A.; Kalia, Y. N.; Guy, R. H., Transdermal drug delivery: overcoming the skin's barrier function. *Pharmaceutical science & technology today* **2000,** *3* (9), 318-326.
26. Schoellhammer, C. M.; Blankschtein, D.; Langer, R., Skin permeabilization for transdermal drug delivery: recent advances and future prospects. *Expert opinion on drug delivery* **2014,** *11* (3), 393-407.
27. Vanbever, R.; Preat, V., In vivo efficacy and safety of skin electroporation. *Advanced drug delivery reviews* **1999,** *35* (1), 77-88.
28. Sersa, G.; Miklavcic, D.; Cemazar, M.; Rudolf, Z.; Pucihar, G.; Snoj, M., Electrochemotherapy in treatment of tumours. *European Journal of Surgical Oncology (EJSO)* **2008,** *34* (2), 232-240.
29. Van Meirvenne, S.; Straetman, L.; Heirman, C.; Dullaers, M.; De Greef, C.; Van Tendeloo, V.; Thielemans, K., Efficient genetic modification of murine dendritic cells by electroporation with mRNA. *Cancer gene therapy* **2002,** *9* (9), 787-797.
30. Sremački, I.; Jurov, A.; Modic, M.; Cvelbar, U.; Wang, L.; Leys, C.; Nikiforov, A. Y., On diagnostics of an annular shape RF plasma jet operating in Ar at atmospheric conditions. *Plasma Sources Science and Technology* **2020**.
31. Sremački, I.; Bruno, G.; Jablonowski, H.; Leys, C.; Nikiforov, A. Y.; Wende, K., Influence of aerosol injection on the liquid chemistry induced by an RF argon plasma jet. *Plasma Sources Science and Technology* **2021**.
32. Sremački, I.; Kos, S. p.; Bošnjak, M. a.; Jurov, A.; Serša, G.; Modic, M.; Leys, C.; Cvelbar, U.; Nikiforov, A., Plasma Damage Control: From Biomolecules to Cells and Skin. *ACS Applied Materials & Interfaces* **2021,** *13* (39), 46303-46316.
33. Park, J. H.; Kim, M.; Shiratani, M.; Cho, A. E.; Choi, E. H.; Attri, P., Variation in structure of proteins by adjusting reactive oxygen and nitrogen species generated from dielectric barrier discharge jet. *Scientific reports* **2016,** *6* (1), 1-14.
34. Van Gaens, W.; Bogaerts, A., Kinetic modelling for an atmospheric pressure argon plasma jet in humid air. *Journal of Physics D: Applied Physics* **2013,** *46* (27), 275201.
35. Ngo Thi, M. H.; Shao, P. L.; Liao, J. D.; Lin, C. C. K.; Yip, H. K., Enhancement of angiogenesis and epithelialization processes in mice with burn wounds through ROS/RNS signals generated by non-thermal N2/Ar micro-plasma. *Plasma Process. Polym.* **2014,** *11* (11), 1076-1088.
36. Livak, K. J.; Schmittgen, T. D., Analysis of relative gene expression data using real-time quantitative PCR and the 2− ΔΔCT method. *methods* **2001,** *25* (4), 402-408.
37. Leduc, M.; Guay, D.; Leask, R.; Coulombe, S., Cell permeabilization using a non-thermal plasma. *New Journal of Physics* **2009,** *11* (11), 115021.
38. Davies, K. J., The broad spectrum of responses to oxidants in proliferating cells: a new paradigm for oxidative stress. *IUBMB life* **1999,** *48* (1), 41-47.

39. Boncler, M.; Różalski, M.; Krajewska, U.; Podsędek, A.; Watala, C., Comparison of PrestoBlue and MTT assays of cellular viability in the assessment of anti-proliferative effects of plant extracts on human endothelial cells. *Journal of pharmacological and toxicological methods* **2014,** *69* (1), 9-16.
40. Smith, M.; Barbenel, J.; Courtney, J.; Grant, M., Novel quantitative methods for the determination of biomaterial cytotoxicity. SAGE Publications Sage UK: London, England: 1992.
41. Yonson, S.; Coulombe, S.; Leveille, V.; Leask, R., Cell treatment and surface functionalization using a miniature atmospheric pressure glow discharge plasma torch. *Journal of Physics D: Applied Physics* **2006,** *39* (16), 3508.
42. Han, G.; Ceilley, R., Chronic wound healing: a review of current management and treatments. *Advances in therapy* **2017,** *34* (3), 599-610.
43. Darby, I. A.; Hewitson, T. D., Fibroblast differentiation in wound healing and fibrosis. *International review of cytology* **2007,** *257*, 143-179.
44. Schmidt, A.; Liebelt, G.; Nießner, F.; von Woedtke, T.; Bekeschus, S., Gas plasma-spurred wound healing is accompanied by regulation of focal adhesion, matrix remodeling, and tissue oxygenation. *Redox biology* **2021,** *38*, 101809.
45. Afratis, N. A.; Nikitovic, D.; Multhaupt, H. A.; Theocharis, A. D.; Couchman, J. R.; Karamanos, N. K., Syndecans–key regulators of cell signaling and biological functions. *The FEBS journal* **2017,** *284* (1), 27-41.
46. Lukes, P.; Dolezalova, E.; Sisrova, I.; Clupek, M., Aqueous-phase chemistry and bactericidal effects from an air discharge plasma in contact with water: evidence for the formation of peroxynitrite through a pseudo-second-order post-discharge reaction of H2O2 and HNO2. *Plasma Sources Science and Technology* **2014,** *23* (1), 015019.
47. Haertel, B.; Von Woedtke, T.; Weltmann, K.-D.; Lindequist, U., Non-thermal atmospheric-pressure plasma possible application in wound healing. *Biomolecules & therapeutics* **2014,** *22* (6), 477.
48. Barrientos, S.; Brem, H.; Stojadinovic, O.; Tomic-Canic, M., Clinical application of growth factors and cytokines in wound healing. *Wound Repair and Regeneration* **2014,** *22* (5), 569-578.
49. Huang, S.; Huang, G., Preparation and drug delivery of dextran-drug complex. *Drug delivery* **2019,** *26* (1), 252-261.
50. Dhaneshwar, S.; Bhilare, N.; Roy, S., Dextran Pharmaceutical Applications. In *Polysaccharides of Microbial Origin: Biomedical Applications*, Springer: 2021; pp 1-28.
51. Ludtke, J. J.; Sebestyén, M. G.; Wolff, J. A., The effect of cell division on the cellular dynamics of microinjected DNA and dextran. *Molecular Therapy* **2002,** *5* (5), 579-588.
52. Larina, I. V.; Evers, B. M.; Esenaliev, R. O., Optimal drug and gene delivery in cancer cells by ultrasound-induced cavitation. *Anticancer research* **2005,** *25* (1A), 149-156.
53. Guignet, E. G.; Meyer, T., Suspended-drop electroporation for high-throughput delivery of biomolecules into cells. *Nature methods* **2008,** *5* (5), 393-395.
54. Stoffels, E.; Sakiyama, Y.; Graves, D. B., Cold atmospheric plasma: charged species and their interactions with cells and tissues. *IEEE Trans. Plasma Sci.* **2008,** *36* (4), 1441-1457.
55. Dobrynin, D.; Fridman, G.; Friedman, G.; Fridman, A., Physical and biological mechanisms of direct plasma interaction with living tissue. *New Journal of Physics* **2009,** *11* (11), 115020.
56. Oinuma, G.; Nayak, G.; Du, Y.; Bruggeman, P. J., Controlled plasma–droplet interactions: A quantitative study of OH transfer in plasma–liquid interaction. *Plasma Sources Science and Technology* **2020,** *29* (9), 095002.
57. Bruggeman, P. J.; Kushner, M. J.; Locke, B. R.; Gardeniers, J. G.; Graham, W.; Graves, D. B.; Hofman-Caris, R.; Maric, D.; Reid, J. P.; Ceriani, E., Plasma–liquid interactions: a review and roadmap. *Plasma sources science and technology* **2016,** *25* (5), 053002.
58. Burlica, R.; Shih, K.-Y.; Locke, B., Formation of H2 and H2O2 in a water-spray gliding arc nonthermal plasma reactor. *Industrial & Engineering Chemistry Research* **2010,** *49* (14), 6342-6349.
59. Rybenkov, V. V.; Vologodskii, A. V.; Cozzarelli, N. R., The effect of ionic conditions on the conformations of supercoiled DNA. I. Sedimentation analysis. *Journal of molecular biology* **1997,** *267* (2), 299-311.

60. Sakai, Y.; Khajoee, V.; Ogawa, Y.; Kusuhara, K.; Katayama, Y.; Hara, T., A novel transfection method for mammalian cells using gas plasma. *Journal of biotechnology* **2006,** *121* (3), 299-308.